

Melt Detection in Antarctic Ice-Sheets Using Spaceborne Scatterometers and Radiometers

Lukas B. Kunz and David G. Long

Brigham Young University Microwave Earth Remote Sensing Laboratory
459 Clyde Building, Provo, UT 84602, Email: lbk2@et.byu.edu and long@ee.byu.edu

Abstract—Backscatter measurements from the SeaWinds on QuikSCAT scatterometer are used to determine periods of surface freeze and melt on Antarctic ice-shelves. A maximum likelihood method is used to infer the daily ice-surface conditions for various study points located on the Ronne, Ross, Larsen, Fimbul, Amery, and Shackleton Ice-shelves.

Criteria for determining the dates of melt-onset and freeze-up for each Austral summer are presented. Validation of the ice-state and melt-onset date estimates is performed by analyzing the corresponding brightness temperature (T_b) measurements from Special Sensor Microwave/Imager (SSM/I) radiometers. QuikSCAT σ° measurements from 1999 through 2003 are analyzed and found to be very useful for determining periods of melt in Antarctic ice-sheets and provide high temporal and spatial resolution ice-state estimates.

I. INTRODUCTION

Recently, longer melt season duration and surface melt ponds on Antarctic ice-shelves have been linked to shelf break-up [1]. Active microwave measurements are very useful in determining annual melt season duration and in observing surface melt pond formation. These measurements are sensitive to changing ice-surface conditions that may indicate the initial signs of shelf retreat. This paper proposes a method for exploiting the sensitivity of dual-polarization scatterometer measurements in order to determine the presence of surface melt on Antarctic ice-shelves.

A maximum likelihood (ML) approach is employed to determine daily ice-state classifications from active microwave backscatter measurements. Yearly maps of melt-onset dates are created and the total number of days classified as melt is also given for each year. It is shown that these ice-state and melt-onset date estimates not only agree with corresponding estimates from passive microwave data but provide added insight from the higher spatial-resolution and increased sensitivity achieved by an active microwave system.

Section II provides background, Section III explains how distributions are calculated for the melt- and non-melt periods, Section IV contains the proposed ML melt detection method and some results, Section V presents the criteria for determining melt-onset and refreeze dates as well as the mapped results, Section VI compares the ML method results with observations from radiometer measurements, and Section VII contains conclusions from this work.

II. BACKGROUND

Spaceborne scatterometers observe the normalized radar backscatter (σ°) of the Earth's surface and are particularly

sensitive to the water content of the illuminated surface. As the amount of liquid water in the snow cover increases, the wet snow at the surface causes a dramatic decrease in the radar backscatter [2]. These backscatter signatures are of primary interest in this analysis.

Brightness temperature measurements from radiometers are sensitive to liquid water in the snow cover. Several algorithms have been implemented to map snowmelt-onset dates on Arctic sea-ice [2] and on the Greenland ice-sheet [3]. Similar algorithms are used in this paper to validate the melt detection results from scatterometer measurements with passive data.

The SeaWinds on QuikSCAT scatterometer operates in Ku-band (13.6 GHz) and has two scanning pencil-beam antennas that measure the 'v'- and 'h'-polarized backscatter. The polar orbiting QuikSCAT provides daily complete coverage of the polar regions regardless of cloud cover or solar illumination. The SSM/I radiometers record T_b measurements on seven channels: dual-polarization at 19.35, 37.0, and 85.5 GHz, and 'v'-pol at 22.235 GHz. Several SSM/I instruments are on board Defense Meteorological Satellite Program (DMSP) satellites, providing full coverage of the polar regions several times each day.

High-resolution images of the measurements from QuikSCAT and the SSM/I sensors produced using the Scatterometer Image Reconstruction (SIR) algorithm [4] are used in the analysis presented. This algorithm combines all passes from a given day to improve the spatial resolution at the expense of some temporal resolution.

III. ICE-STATE DISTRIBUTION ESTIMATIONS

To observe the intra- and inter-shelf radar response characteristics, various points are selected from each of the major ice-shelves. The yearly and seasonal variations in the measured backscatter values for each point are observed.

QuikSCAT's dual-polarization backscatter measurements (σ_H° and σ_V°) are very correlated but exhibit different sensitivities to the presence of liquid water. This is observed from the 'quasi' polarization ratio (PR) defined by

$$PR = \sigma_V^\circ - \sigma_H^\circ,$$

where the values are in dB. This is not a true polarization ratio since the 'v'- and 'h'-pol measurements are from different incidence angles. In general, σ_V° is ~ 1 dB below the σ_H° values.

From the time-series in Figure 1 we see that PR fluctuates much more during each Austral summer than during the

winter. This results from the greater sensitivity of 'h'-pol backscatter to liquid water in the snow cover than 'v'-pol backscatter. This time-series is typical of most areas that experience surface melting. Backscatter values for locations with no melt events are nearly constant with time.

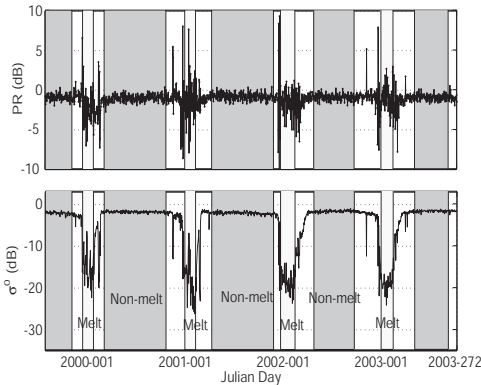


Fig. 1. (top) PR and (bottom) σ_H^o time-series for study point 7 ($67^\circ S$, $61.5^\circ W$) on the Larsen Ice-shelf. During each year, contiguous periods (shown as shaded and unshaded boxes) of alternating melt and non-melt are identified. Each period's mean and covariance are empirically computed and used in ML ice-state estimations.

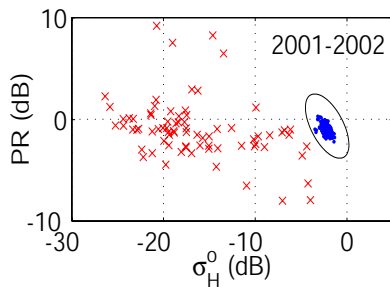


Fig. 2. Scatterplot of σ_H^o vs. PR for point 7 for 2001-02. Other years from 1999-2003 are similar. The ellipse is the contour of equal Mahalanobis distance from the melt- and non-melt mean values (see text).

Figure 2 shows a scatterplot of σ_H^o vs. PR for point 7. Note the concentration of non-melt values around the point $(-2\text{dB}, -1\text{dB})$. The remaining values, which are during summer melt, are loosely grouped. This suggests that the backscatter and PR observations may be modeled as random variables with separate means and covariances for melt and non-melt periods. For simplicity a gaussian distribution is assumed and the mean vector and covariance matrix during each specified period in Figure 1 are computed.

Of particular interest is the northern-most study point on the Larsen Ice-shelf. The time-series for this point varies significantly more than for the other peninsular points. Recently, this region has become the subject of interest for observing and understanding the causes and impacts of ice-shelf breakup [1]. In Section V the scatterometer observations for this location are shown to be more sensitive to changing shelf-surface conditions than passive microwave observations.

IV. MAXIMUM LIKELIHOOD ESTIMATION OF ICE-STATES

Given the scatterometer measurements, the daily ice-state for each location is estimated using the maximum likelihood method. Forming the log-likelihood ratio simplifies the melt hypothesis test to a comparison of weighted norms, the so-called Mahalanobis distance,

$$\phi(\mathbf{x}) = \begin{cases} 1 & \|\mathbf{x} - \mathbf{m}_1\|_{\mathbf{R}_1}^{-1} < \|\mathbf{x} - \mathbf{m}_0\|_{\mathbf{R}_0}^{-1} + \log \frac{|\mathbf{R}_0|}{|\mathbf{R}_1|} \\ 0 & \text{otherwise,} \end{cases}$$

where \mathbf{R}_0 and \mathbf{R}_1 are the respective covariance matrices for non-melt and melt conditions, \mathbf{x} is a two-element vector of observed σ_H^o and PR values, and \mathbf{m}_0 and \mathbf{m}_1 contain the estimated mean σ_H^o and PR values for the respective ice-states.

This test is performed on the daily σ^o values for each study point from 1999 through 2003. Each day is classified independently so the result from one day does not influence the ice-state estimation for any other day. The data is divided into yearly segments and the mean and covariance from each given year are used in the ML test. For points that exhibit very few days of melting the empirically computed covariance matrices may be ill-conditioned. In such cases the covariance from a nearby point is used instead. Figure 3 illustrates the results of the ML ice-state estimation for points 7 and 19. The melt classification results for other points are similar (see Table I).

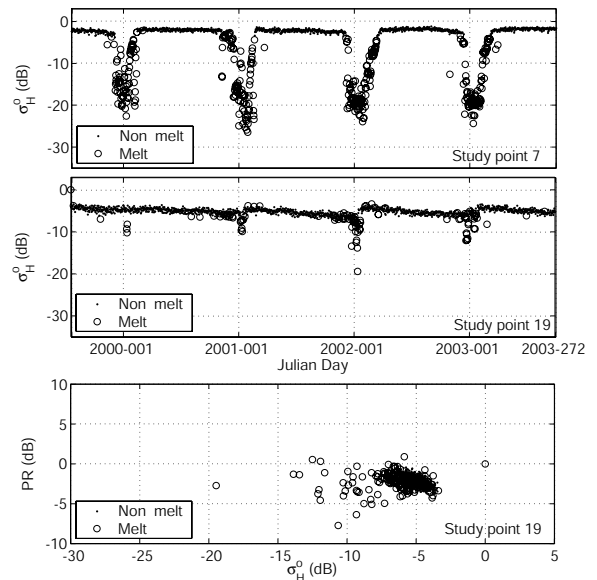


Fig. 3. (top) Time-series for point 7, (center) time-series for point 19 ($70.5^\circ S$, $1^\circ E$) and (bottom) scatterplot for point 19 with resulting ML method surface-melt estimates.

The method performs well for location 7 since periods of reduced backscatter are classified as melt. There are, however, some days during the summer with backscatter close to the winter mean value that are selected as melt events. Study point 19 shows that some potentially false melt classifications occur when refrozen snow backscatter measurements are higher than

the winter non-melt values (Figure 3). This happens when the backscatter values lie to the right of the decision boundary in the σ_H^o vs. PR scatterplot.

A slight modification to the decision boundary can compensate for this problem; however, since such measurements represent a distinct deviation from the normal non-melt conditions, the points classified as melt that have higher backscatter values should be identified and analyzed further. Possible explanations for this behavior include a dramatic refreeze event, the formation of frost flowers, or a significant accumulation event, among others.

V. DETERMINING MELT-ONSET AND REFREEZE DATES

Determining the dates of melt-onset and refreeze is important in understanding the inter-annual variability of surface melt in Antarctica. Previous efforts to map these events have focused on Arctic and Antarctic sea-ice.

Using the ML method we propose that the melt-onset date be chosen as the beginning of a three-day period of consecutive melt classifications and the refreeze date is selected as the start of a period of no melt classifications for at least 7 days. Figure 4 contains maps of the melt-onset date estimates for 2000-01 over the Antarctic peninsula while Figure 4 maps the total number of days classified as melt events during 2000-01 for the peninsula. For each pixel in the images the means and covariances from the nearest study point are used in the ML ice-state classification. Only locations below 100m in elevation are considered.

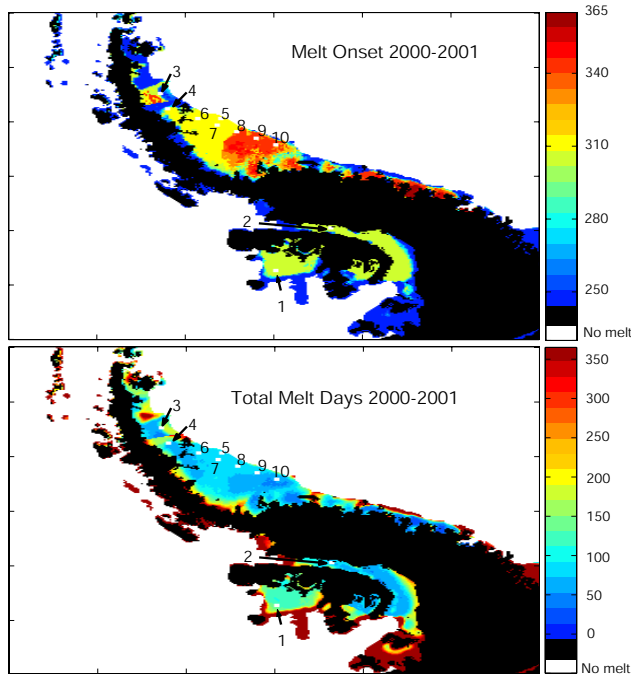


Fig. 4. (top) Melt-onset dates (Julian Day of 2000) and (bottom) total melt days for the Larsen Ice-shelf for Austral summer 2000-01. The 10 study points in this region are indicated.

For the discussion of these melt maps we follow the terminology used by Vaughan and Doake [5]: the northernmost

section of the Larsen Ice-shelf (just north of study point 3) is termed the Larsen “A”, the section covered by points 3 and 4 is the Larsen “B”, and points 5-10 span the Larsen “C”.

From Figure 4 we see that the Larsen A experiences a very early melt onset and over 300 days of melt each year. This is expected since the Larsen A disintegrated in 1995, thus removing all multi-year ice from the area [1]. The boundary between the Larsen A and Larsen B ice-shelves is marked by an abrupt change in the results from the melt-total and melt-onset maps for each year. The Larsen B melt season begins much later and ends earlier than for the Larsen A.

The Larsen C experiences significant melt much later than the Larsen A and B for the 2000-01 melt-season. Examining 1999-2003 the total melt days for over the Larsen C is consistent from year to year, but for 2000-01 the southern portion of the shelf begins its melt season more than a month later than the northern part. This may indicate that the northern section is less stable and susceptible to break-up.

The ML method melt-onset and melt season duration results are realistic. The method consistently classifies melt over contiguous areas and some interesting features are observed in the variations of the melt seasons from year to year. To determine the validity of this melt detection method passive microwave measurements are analyzed using previous methods and the results are given in the next section.

VI. VALIDATION USING RADIOMETER DATA

Passive microwave measurements have previously been used to detect melt on Arctic sea-ice and the Greenland ice-sheet. The results from three melt detection methods using SSM/I data are compared to the ML method classifications using QuikSCAT data.

Anderson [2] used the horizontal range,

$$HR = T_b(19H) - T_b(37H) < 2K, \quad (1)$$

to determine melting events on Arctic sea-ice. $T_b(19H)$ is the ‘h’-pol 19 GHz channel value and $T_b(37H)$ is the ‘h’-pol 37 GHz channel value for a given location.

Abdalati and Steffen [6] used the cross-gradient polarization ratio (XPGR) to detect melt over Greenland, i.e. melt is detected when

$$XPGR = \frac{T_b(19H) - T_b(37V)}{T_b(19H) + T_b(37V)} > -0.0158. \quad (2)$$

A method for determining melt on the Greenland ice-sheet proposed by Ashcraft and Long [3], hereafter $T_b\text{-}\alpha$, uses a threshold set between the mean winter brightness temperature value (T_b^{dry}) and the brightness temperature for wet snow (T_b^{wet}). Melt is classified for

$$T_b > \alpha T_b^{dry} + (1 - \alpha) T_b^{wet} \quad (3)$$

where $T_b^{wet} = 273K$, $\alpha = 0.46$, and T_b is the ‘v’-pol 19 GHz channel value [3].

Figure 5 shows a time-series of SSM/I and QuikSCAT data at two locations. Note that when the backscatter decreases significantly there is usually an accompanying rise in

brightness temperature measurements. The data for point 3 in Figure 5 reveals a deviation from this pattern. The drop in backscatter during the 2001-2002 Austral summer corresponds to varying responses in the T_b values for each SSM/I channel. Since passive microwave observations are more subject to changing atmospheric conditions, the discrepancy between the sensors at this location may be due to atmospheric effects. The variation in responses between the SSM/I channels are due to the different operating frequencies and polarizations. Higher-frequency channels are effected more by interference from the atmosphere.

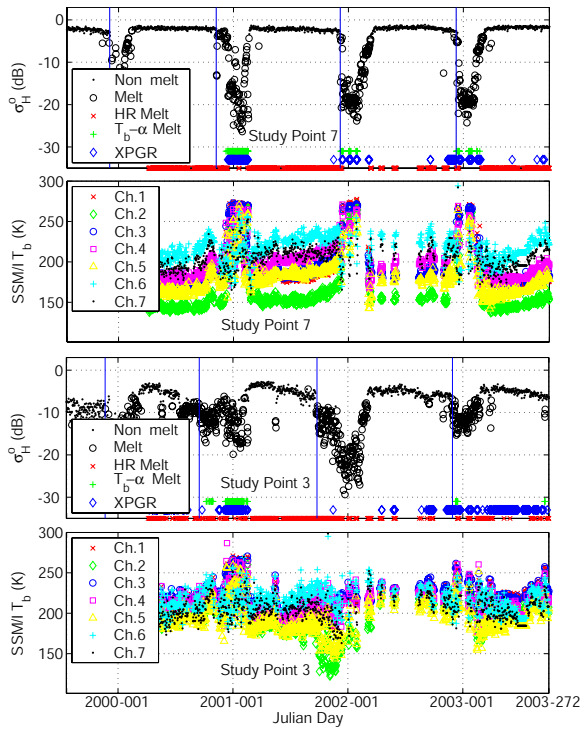


Fig. 5. Results from the ML and SSM/I methods for point 7 (top two plots) and point 3 (65.35°S, 60.5°W) (bottom two plots). Vertical lines mark the melt-onset dates from the ML method. ML, T_b - α , and XPGR melt classifications are consistent for point 7 but differ for point 3 where T_b - α and XPGR miss the melt season of 01-02 and diverge for 02-03. The HR method appears to be invalid for this region. (see text)

The results of the HR, XPGR, and T_b - α melt algorithms are also shown in Figure 5 along the bottom of the σ^0 time-series. The HR method classifies nearly every day as melt for each of the 25 study points. This indicates that the HR method is not portable for use in melt detection in Antarctica. The ML, XPGR, and T_b - α results are more consistent, with the ML method generally resulting in more days classified as melt than the T_b - α method. XPGR results vary much more from year to year than the other methods.

In some cases the ML method appears to be more sensitive to melt conditions than the methods using passive microwave data. This is evident in the results for study point 3 in Figure 5. The T_b - α method does not count any melt events during the 2001-02 summer; however, the backscatter time-series clearly indicates substantial melting and the ML method

appropriately identifies many days of surface melt. XPGR sporadically identifies a few days as melt during this period and overestimates the number of melt events for the 2002-03 summer and winter of 2003.

The total number of melt days and the melt-onset dates from the ML method for the 10 study points over the peninsula during each year of the study are given in Table I. The melt-onset dates calculated by the ML algorithm are usually a few days prior to the first day of melt detected by XPGR and T_b - α . For most of the study points it is observed that when each of the ML, XPGR, and T_b - α methods detect melt during a given melt season the melt-onset dates for the ML and T_b - α methods are within a few days while the XPGR dates vary considerably.

TABLE I
ML METHOD MELT-ONSET DATES (JULIAN DAY) AND TOTAL NUMBER OF MELT DAYS FOR EACH YEAR OVER THE ANTARCTIC PENINSULA.

Point	1999-00 Onset/Total	2000-01 Onset/Total	2001-02 Onset/Total	2002-03 Onset/Total
1	279 / 153	306 / 131	270 / 103	332 / 097
2	311 / 112	307 / 070	345 / 082	332 / 081
3	324 / 149	257 / 133	266 / 159	331 / 096
4	322 / 099	308 / 059	334 / 094	299 / 078
5	337 / 075	309 / 089	338 / 099	341 / 089
6	324 / 083	308 / 079	334 / 099	341 / 084
7	337 / 075	309 / 087	338 / 098	341 / 091
8	337 / 060	341 / 078	338 / 097	341 / 085
9	337 / 054	341 / 073	343 / 091	345 / 087
10	337 / 054	341 / 056	343 / 078	345 / 083

VII. CONCLUSIONS

The maximum likelihood ML melt detection algorithm using QuikSCAT dual-polarization measurements is shown to be a promising method for detecting surface melt. Melt classifications using this method are spatially consistent and the melt-onset date estimates correspond to the beginning of periods with greatly reduced backscatter. The backscatter observed by QuikSCAT is at a much finer resolution than the radiometer T_b measurements, allowing for more precise observation of spatially-varying surface melt.

REFERENCES

- [1] T. A. Scambos and C. Hulbe and M. Fahnestock and J. Bohlander, "The link between climate warming and break-up of ice shelves in the Antarctic Peninsula", *Journal of Glaciology*, vol. 46, no. 154, 2000.
- [2] R. R. Forster and D. G. Long and K. C. Jezek and S. D. Drobot and M. R. Anderson, "The onset of Arctic sea-ice snowmelt as detected with passive- and active-microwave remote sensing", *Annals of Glaciology*, vol. 33, pp. 85-93, 2001.
- [3] I. Ashcraft and D. G. Long, "Comparison of methods for melt detection over Greenland using active and passive microwave measurements", *IEEE Transactions on Geoscience and Remote Sensing*, 2004, in review.
- [4] D. G. Long and D. Daum, "Spatial resolution enhancement of SSM/I data", *IEEE Transactions on Geoscience and Remote Sensing*, vol. 36, pp. 407-417, 1997.
- [5] D. G. Vaughan and C. S. M. Doake, "Recent atmospheric warming and retreat of ice shelves on the Antarctic Peninsula", *Nature*, vol. 379, no. 6563, pp. 328-331, 1996.
- [6] W. Abdalati and K. Steffen, "Greenland ice sheet melt extent: 1979-1999", *Journal of Geophysical Research*, vol. 106, no. D24, pp. 33983-33988, December 2001.